antioxidants

MDPI

Article

The Balancing of Peroxynitrite Detoxification between Ferric Heme-Proteins and CO_2: The Case of Zebrafish Nitrobindin

Giovanna De Simone [1,†], Andrea Coletta [1,†], Alessandra di Masi [1], Massimo Coletta [2,*] and Paolo Ascenzi [1,*]

[1] Dipartimento di Scienze, Università Roma Tre, 00146 Roma, Italy
[2] IRCCS Fondazione Bietti, 00198 Roma, Italy
* Correspondence: massimiliano.coletta@fondazionebietti.it (M.C.); paolo.ascenzi@uniroma3.it (P.A.)
† These authors contributed equally to this work.

Abstract: Nitrobindins (Nbs) are all-β-barrel heme proteins and are present in prokaryotes and eukaryotes. Although their function(s) is still obscure, Nbs trap NO and inactivate peroxynitrite. Here, the kinetics of peroxynitrite scavenging by ferric *Danio rerio* Nb (*Dr*-Nb(III)) in the absence and presence of CO_2 is reported. The *Dr*-Nb(III)-catalyzed scavenging of peroxynitrite is facilitated by a low pH, indicating that the heme protein interacts preferentially with peroxynitrous acid, leading to the formation of nitrate (~91%) and nitrite (~9%). The physiological levels of CO_2 dramatically facilitate the spontaneous decay of peroxynitrite, overwhelming the scavenging activity of *Dr*-Nb(III). The effect of *Dr*-Nb(III) on the peroxynitrite-induced nitration of L-tyrosine was also investigated. *Dr*-Nb(III) inhibits the peroxynitrite-mediated nitration of free L-tyrosine, while, in the presence of CO_2, *Dr*-Nb(III) does not impair nitro-L-tyrosine formation. The comparative analysis of the present results with data reported in the literature indicates that, to act as efficient peroxynitrite scavengers in vivo, i.e., in the presence of physiological levels of CO_2, the ferric heme protein concentration must be higher than 10^{-4} M. Thus, only the circulating ferric hemoglobin levels appear to be high enough to efficiently compete with CO_2/HCO_3^- in peroxynitrite inactivation. The present results are of the utmost importance for tissues, like the eye retina in fish, where blood circulation is critical for adaptation to diving conditions.

Keywords: *Danio rerio* heme-protein; effect of CO_2; kinetics; peroxynitrite detoxification; tyrosine protection; zebrafish nitrobindin

Citation: De Simone, G.; Coletta, A.; di Masi, A.; Coletta, M.; Ascenzi, P. The Balancing of Peroxynitrite Detoxification between Ferric Heme-Proteins and CO_2: The Case of Zebrafish Nitrobindin. *Antioxidants* **2022**, *11*, 1932. https://doi.org/10.3390/antiox11101932

Academic Editors: Stanley Omaye and Brandon Reeder

Received: 27 July 2022
Accepted: 22 September 2022
Published: 28 September 2022

1. Introduction

Nitrosative stress plays a key role in the etiology of human diseases, such as atherosclerosis, inflammation, cancer, and neurological diseases, being particularly relevant in the onset of retinopathies and glaucoma [1–3]. In fact, reactive nitrogen species (RNS) can cause protein, DNA, and lipid nitration, impairing their functions [4–11]. One of the most potent biological nitrosative agents is peroxynitrite ($ONOO^-$), which is produced when nitric oxide ($^{\bullet}NO$) and superoxide ($^{\bullet}O_2^-$) are combined at extremely rapid rates [4,5,9–13]. $ONOO^-$ diffuses through membrane anion channels as well as the conjugated peroxynitrous acid ONOOH (pK_a = 6.9) [13]. $ONOO^-$ is relatively stable, while ONOOH decays rapidly, with an apparent half-life of 1-2 s at physiological pH, yielding ~70% nitrate (NO_3^-) and H^+, and ~30% nitrogen dioxide ($^{\bullet}NO_2$) and hydroxyl ($^{\bullet}OH$) radicals via the homolysis of the O–O bond. The secondary reactions of $^{\bullet}NO_2$ and $O^{\bullet-}$ lead to NO_2^- and O_2 [4,9–13]. $ONOO^-$ reacts with biomolecules mainly by a direct reaction or immediately after ONOOH is homolyzed to $^{\bullet}NO_2$ and $^{\bullet}OH$ [4,9–13].

At the end of the last century, carbon dioxide (CO_2) was reported to react with $ONOO^-$ [14,15]. Since the CO_2 concentration is relatively high in vivo (~1.2×10^{-3} M at physiological pH in equilibrium with ~2.4×10^{-2} M HCO_3^- with a $pK_a \approx 6.3$ at 25.0 °C), most of the $ONOO^-$ rapidly reacts with the CO_2/HCO_3^- species (depending on pH),

leading mostly to the formation of 1-carboxylato-2-nitrosodioxidane adduct ($ONOOCO_2^-$), which displays an apparent half-life of 0.5–3 ms. This compound further decays (via homolysis of the O–O bond), yielding the reactive species trioxocarbonate$^{\bullet-}$ ($CO_3^{\bullet-}$) and $^{\bullet}NO_2$ (3% to 35%), which then proceed towards CO_2 and NO_3^- (or by direct yielding of NO_3^- and CO_2 (65% to 90%) [9,11–21]). As a whole, the complexity of the peroxynitrite inactivation mechanism can be sketched, as is shown in Scheme 1 [13,22–41], where *Dr*-Nb(III) represents the contribution of heme proteins.

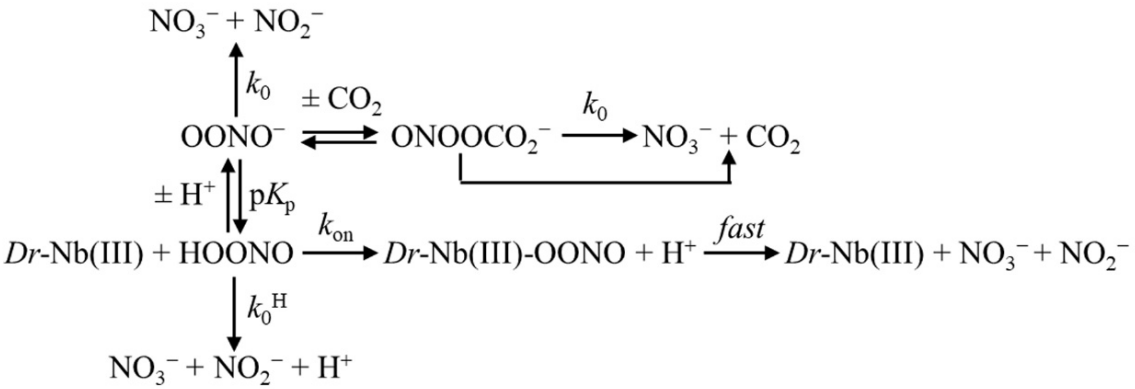

Scheme 1. *Dr*-Nb(III)-mediated isomerization of peroxynitrite in the absence and presence of CO_2 (representing the $CO_2/HCO_3^-/CO_3^{2-}$ system). The disappearance of the pH-dependent $ONOO^-$/ONOOH species is characterized by the absorption decrease at 302 nm. For the sake of clarity, only the final products of the peroxynitrite inactivation mechanisms (indicated by k_0 and k_0^H) are reported, while the intermediate species are described in the text.

Moreover, the reaction of $ONOO^-$ with $CO_2/HCO_3^-/CO_3^{2-}$ redirects the $ONOO^-$/ONOOH-based oxidation of aromatic and aliphatic amino acid residues, facilitating the nitration of tyrosine and tryptophan and limiting the oxidation of methionine and cysteine [5,9–15,20,21,42–45]. Remarkably, $^{\bullet}NO_2$ and $CO_3^{\bullet-}$ radicals are much stronger oxidant species than their precursors $^{\bullet}NO$, $O_2^{\bullet-}$, and $ONOO^-$/ONOOH [9–13,20,21,46].

Tyrosine nitration through the peroxynitrite pathway (see Scheme 1) is operative in most fish, including zebrafish (*Danio rerio*), under stressed conditions [47,48]. Further, the effect of the enrichment of CO_2 in the atmosphere brings about the raising of CO_2 levels also in the oceans [49]. Although the increased levels of CO_2 create only limited behavioral effects, they may significantly affect the body response to external insults. In addition, the increased concentration of CO_2 in the blood is of particular relevance in fish, for which retinal circulation is of crucial importance due to the high hydrostatic pressure of the environment where they live [50,51].

Here, the kinetics of $ONOO^-$/ONOOH (hereafter peroxynitrite) inactivation by all-β-barrel ferric *Danio rerio* nitrobindin (*Dr*-Nb(III)), in the absence and presence of CO_2, are reported and analyzed in parallel with those of all-α-helical globins. The present results open a question on the competition between the protecting activity of heme proteins (which inactivate the damaging reactions of peroxynitrite on L-tyrosine nitration) and the non-protecting action of CO_2/HCO_3^-, which indeed depends on the levels of ferric heme-proteins. Thus, the levels (and the scavenging activity) of most heme proteins might be too low to act as peroxynitrite scavengers in vivo; only circulating ferric hemoglobin (Hb(III)) levels appear to be high enough to efficiently compete with $CO_2/HCO_3^-/CO_3^{2-}$ in peroxynitrite inactivation.

2. Materials and Methods

2.1. Materials

Dr-Nb(III) was cloned, expressed, and purified as already reported [52]. The *Dr*-Nb(III) concentration was determined spectrophotometrically by measuring the absorbance

at 407 nm (ε = 1.57 × 10^5 M^{-1} cm^{-1}) [52]. Apo-*Dr*-Nb was prepared, as already reported [53]. Peroxynitrite was obtained from Cayman Chemical (Ann Arbor, MI, USA). The concentration of peroxynitrite was determined spectrophotometrically at 302 nm (ε = 1.705 × 10^3 M^{-1} cm^{-1}) [12]. L-tyrosine (obtained from Merck KGaA, Darmstadt, Germany) was dissolved in 5.0 × 10^{-2} M Bis-Tris propane buffer, at pH 7.0 and 22.0 °C; the final L-tyrosine concentration was 1.0 × 10^{-4} M [25,30,36,39]. All the other chemicals were purchased from Merck KGaA (Darmstadt, Germany). All chemicals were of analytical grade and were used without further purification.

2.2. Methods

In the absence and presence of CO_2, peroxynitrite isomerization by *Dr*-Nb(III) and apo-*Dr*-Nb was investigated at pH 5.8, 7.0, and 8.5 (5.0 × 10^{-2} M Bis-Tris propane buffer) and 22.0 °C, under anaerobic conditions. In the presence of CO_2, peroxynitrite isomerization by *Dr*-Nb(III) and apo-*Dr*-Nb was investigated by adding $NaHCO_3$ (final concentration, 5.0 × 10^{-1} M) to the *Dr*-Nb(III) and apo-*Dr*-Nb solutions; this $NaHCO_3$ concentration corresponds to different concentrations of CO_2, HCO_3^-, and CO_3^{2-} depending on pH. After the addition of $NaHCO_3$, the *Dr*-Nb(III) and apo-*Dr*-Nb solutions were allowed to equilibrate for at least 5 min; then, the pH was readjusted to the desired pH if needed [25,27,28,30,36,39].

Peroxynitrite isomerization by *Dr*-Nb(III) and apo-*Dr*-Nb was investigated via rapid mixing of the *Dr*-Nb(III) and apo-*Dr*-Nb solutions (final concentration ranging between 5.0 × 10^{-6} M and 3.5 × 10^{-5} M) with the peroxynitrite solution (final concentration ranging between 2.5 × 10^{-5} M and 2.0 × 10^{-4} M); no gaseous phase was present. Peroxynitrite isomerization was monitored at 302 nm [9,12,25–27,30,36,39] by the SFM-20/MOS-200 rapid-mixing stopped-flow apparatus (BioLogic Science Instruments, Claix, France); the light path of the observation chamber was 10 mm and the dead-time was 1.3 ms.

Values of the pseudo-first-order rate constant for peroxynitrite isomerization by *Dr*-Nb(III) and apo-*Dr*-Nb (i.e., k_{obs}) were determined according to Equation (1) [13,22–41,54,55]:

$$[\text{peroxynitrite}]_t = [\text{peroxynitrite}]_i \times e^{-k\text{obs} \times t} \quad (1)$$

Values of the second-order rate constant for peroxynitrite isomerization by *Dr*-Nb(III) (i.e., k_{on}), and of the first-order rate constant for the spontaneous decay of peroxynitrite (i.e., k_0), were obtained from the dependence of k_{obs} on the *Dr*-Nb(III) concentration, according to Equation (2) [13,22–41,54,55]:

$$k_{obs} = k_{on} \times [Dr\text{-Nb(III)}] + k_0 \quad (2)$$

The reaction of peroxynitrite with L-tyrosine was investigated at pH 7.0 and 22.0 °C, as reported elsewhere. The relative nitro-L-tyrosine yield (%) corresponds to: (yield with added *Dr*-Nb(III) or apo-*Dr*)/(yield with no *Dr*-Nb(III) or apo-*Dr*-Nb) × 100 [13,25,30,34–36,39,55,56].

The percentage of NO_3^- and NO_2^- obtained from peroxynitrite isomerization was determined spectrophotometrically at 543 nm by using the Griess reagent and vanadium(III) chloride (VCl_3) to catalyze the conversion of NO_3^- to NO_2^-, according to literature [25,30,36,39,56].

Kinetic data were analyzed using the GraphPad Prism program, version 5.03 (GraphPad Software, San Diego, CA, USA). The results are given as the mean values of at least four experiments plus and minus the standard deviation. Data were analyzed using GraphPad Prism 6 (GraphPad Software Inc., San Diego, CA, USA) and were expressed as mean values ± standard deviation (SD). Statistical analysis was performed using either the Student's *t*-test or the one-way ANOVA comparison test (* $p < 0.05$; ** $p < 0.01$; *** $p < 0.001$; **** $p < 0.0001$).

3. Results and Discussion

In the absence and presence of CO_2, the absorbance at 302 nm decreases upon mixing the *Dr*-Nb(III), apo-*Dr*-Nb, and peroxynitrite solutions over the whole pH range explored.

According to the literature [13,22–41,54,55], this reflects peroxynitrite isomerization. No absorbance spectroscopic changes were observed in the Soret region.

Under all the experimental conditions, the time course of peroxynitrite isomerization in the absence and presence of *Dr*-Nb(III), apo-*Dr*-Nb, and CO_2 was fitted to a single-exponential decay for more than 93% of its course, according to Equation (1) (Figures 1–3, panels A and B). The values of the pseudo-first-order rate constant for peroxynitrite isomerization catalyzed by *Dr*-Nb(III) (i.e., k_{obs}) increase with the heme protein concentration (Figures 1–3, panels C and D). Previous experiments have shown that, once bound to a heme protein (likely as Fe(III)-ONOOH), peroxynitrite isomerizes to NO_3^- at a rate of ~70 s^{-1} [13]. Therefore, since the values of k_{obs} range between 1×10^{-1} s^{-1} and 8 s^{-1} (Figures 1–3, panel C), they indicate that, under our conditions, the formation of the *Dr*-Nb(III)-OONOH species represents the rate-limiting step of the catalytic process. Notably, the *Dr*-Nb(III)-OONOH conversion to *Dr*-Nb(III) and NO_3^- is faster by at least 10-fold than the formation of the *Dr*-Nb(III)-OONOH complex.

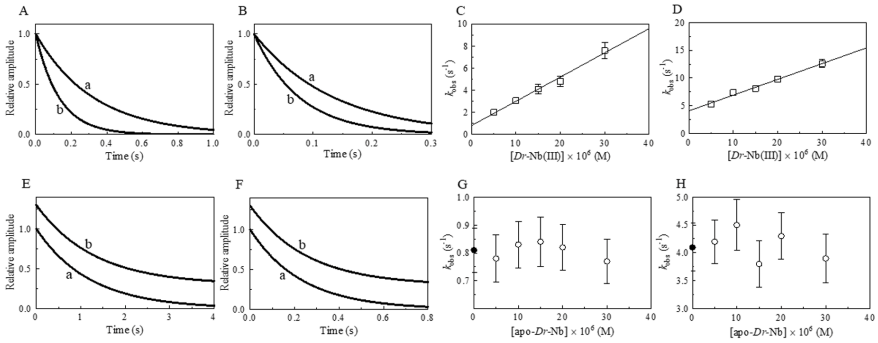

Figure 1. Effect of *Dr*-Nb(III) on the kinetics for peroxynitrite isomerization, at pH 5.8 and 22.0 °C. (**A**) Averaged time courses of the *Dr*-Nb(III)-catalyzed isomerization of peroxynitrite in the absence of CO_2. The time course analysis, according to Equation (1), allowed us to determine the following values of k_{obs}: trace a, 3.1 s^{-1}, R = 0.998; trace b, 7.6 s^{-1}, R = 0.998. The *Dr*-Nb(III) concentration was: trace a, 1.0×10^{-5} M; trace b, 3.0×10^{-5} M. (**B**) Averaged time courses of the *Dr*-Nb(III)-catalyzed isomerization of peroxynitrite in the presence of CO_2. The time course analysis, according to Equation (1), allowed us to determine the following values of k_{obs}: trace a, 7.4 s^{-1}, R = 0.999; trace b, 1.3×10^{1} s^{-1}, R = 0.998. The *Dr*-Nb(III) concentration was: trace a, 1.0×10^{-5} M; trace b, 3.0×10^{-5} M. The CO_2 concentration was 1.2×10^{-3} M. (**C**) Dependence of k_{obs} on the concentration of *Dr*-Nb(III) in the absence of CO_2. Data were analyzed according to Equation (2) with $k_{on} = 2.2 \times 10^5$ M^{-1} s^{-1} and $k_0 = 8.1 \times 10^{-1}$ s^{-1}; R = 0.989, p = 0.0006. (**D**) Dependence of k_{obs} on the concentration of *Dr*-Nb(III) in the presence of CO_2. Data obtained were analyzed according to Equation (2) with $k_{on} = 2.8 \times 10^5$ M^{-1} s^{-1} and k_0 = 4.1 s^{-1}; R = 0.991, p = 0.0005. (**E**) Averaged time courses of peroxynitrite isomerization by apo-*Dr*-Nb in the absence of CO_2. The time course analysis, according to Equation (1), allowed us to determine the following values of k_{obs}: trace a, 8.3×10^{-1} s^{-1}; trace b, 7.7×10^{-1} s^{-1}. The apo-*Dr*-Nb concentration was: trace a, 1.0×10^{-5} M; trace b, 3.0×10^{-5} M. For clarity, trace b has been up-shifted of 0.3 units. (**F**) Averaged time courses of peroxynitrite isomerization by apo-*Dr*-Nb in the presence of CO_2. The time course analysis, according to Equation (1), allowed us to determine the following values of k_{obs}: trace a, 4.3 s^{-1}; trace b, 3.9 s^{-1}. The apo-*Dr*-Nb concentration was: trace a, 1.0×10^{-5} M; trace b, 3.0×10^{-5} M. For clarity, trace b has been up-shifted of 0.3 units. The CO_2 concentration was 1.2×10^{-3} M. (**G**) Dependence of k_{obs} on the concentration of apo-*Dr*-Nb in the absence of CO_2. The symbol on the ordinate indicates the value of k_0: 8.0×10^{-1} s^{-1}. The average value of k_{obs} obtained in the presence of apo-*Dr*-Nb is: 8.1×10^{-1} s^{-1}. (**H**) Dependence of k_{obs} on the concentration of apo-*Dr*-Nb in the presence of CO_2. The symbol on the ordinate indicates the value of k_0: 4.1 s^{-1}. The average value of k_{obs} obtained in the presence of apo-*Dr*-Nb and CO_2 is: 4.1 s^{-1}. In panels G and H, the differences among the k_{obs} values are not statistically significant. The peroxynitrite concentration was 2.0×10^{-4} M. The HCO_3^- concentration was 5.0×10^{-1} M. Where not shown, the standard deviation is smaller than the symbol.

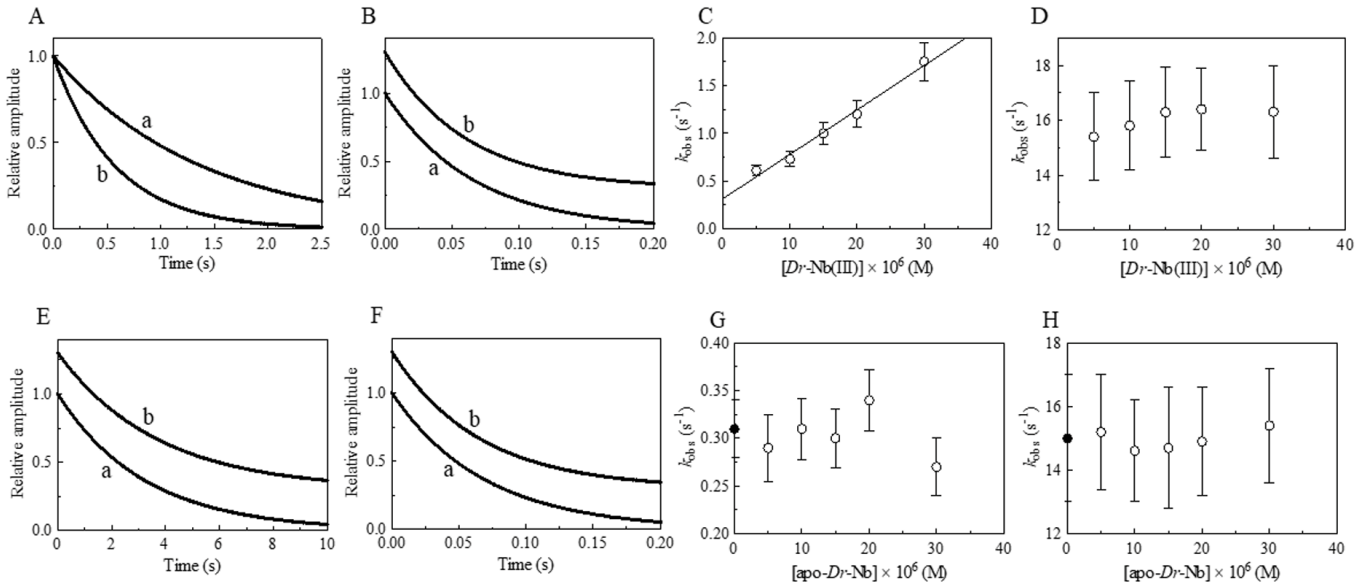

Figure 2. Effect of *Dr*-Nb(III) on the kinetics for peroxynitrite isomerization, at pH 7.0 and 22.0 °C. (**A**) Averaged time courses of the *Dr*-Nb(III)-catalyzed isomerization of peroxynitrite in the absence of CO_2. The time course analysis according to Equation (1) allowed us to determine the following values of k_{obs}: trace a, 7.3×10^{-1} s^{-1}, $R = 0.998$; trace b, 1.8 s^{-1}, $R = 0.999$. The *Dr*-Nb(III) concentration was: trace a, 1.0×10^{-5} M; trace b, 3.0×10^{-5} M. (**B**) Averaged time courses of the *Dr*-Nb(III)-catalyzed isomerization of peroxynitrite in the presence of CO_2. The time course analysis according to Equation (1) allowed us to determine the following values of k_{obs}: trace a, 1.5×10^{1} s^{-1}, $R = 0.999$; trace b, 1.7×10^{1} s^{-1}, $R = 0.998$. The *Dr*-Nb(III) concentration was: trace a, 1.0×10^{-5} M; trace b, 3.0×10^{-5} M. The CO_2 concentration was 1.2×10^{-3} M. For clarity, trace b has been up-shifted of 0.3 units. (**C**) Dependence of k_{obs} on the concentration of *Dr*-Nb(III) in the absence of CO_2. Data were analyzed according to Equation (2) with $k_{on} = 4.7 \times 10^{4}$ M^{-1} s^{-1} and $k_0 = 3.1 \times 10^{-1}$ s^{-1}; $R = 0.989$, $p = 0.0006$. (**D**) Dependence of k_{obs} on the concentration of *Dr*-Nb(III) in the presence of CO_2. (**E**) Averaged time courses of peroxynitrite isomerization by apo-*Dr*-Nb in the absence of CO_2. The time course analysis according to Equation (1) allowed us to determine the following values of k_{obs}: trace a, 3.1×10^{-1} s^{-1}; trace b, 2.7×10^{-1} s^{-1}. The apo-*Dr*-Nb concentration was: trace a, 1.0×10^{-5} M; trace b, 3.0×10^{-5} M. For clarity, trace b has been up-shifted of 0.3 units. (**F**) Averaged time courses of peroxynitrite isomerization by apo-*Dr*-Nb in the presence of CO_2. The time course analysis according to Equation (1) allowed us to determine the following values of k_{obs}: trace a, 1.5×10^{1} s^{-1}; trace b, 1.6×10^{1} s^{-1}. The apo-*Dr*-Nb concentration was: trace a, 1.0×10^{-5} M; trace b, 3.0×10^{-5} M. For clarity, trace b has been up-shifted of 0.3 units. The CO_2 concentration was 1.2×10^{-3} M. (**G**) Dependence of k_{obs} on the concentration of apo-*Dr*-Nb in the absence of CO_2. The symbol on the ordinate indicates the value of k_0: 3.1×10^{-1} s^{-1}. The average value of k_{obs} obtained in the presence of apo-*Dr*-Nb is: 3.0×10^{-1} s^{-1}. (**H**) Dependence of k_{obs} on the concentration of apo-*Dr*-Nb in the presence of CO_2. The symbol on the ordinate indicates the value of k_0: 1.5×10^{1} s^{-1}. The average value of k_{obs} obtained in the presence of apo-*Dr*-Nb and CO_2 is: 1.5×10^{1} s^{-1}. In panels D, G, and H, the differences among the k_{obs} values are not statistically significant. The peroxynitrite concentration was 2.0×10^{-4} M. The HCO_3^- concentration was 5.0×10^{-1} M. Where not shown, the standard deviation is smaller than the symbol.

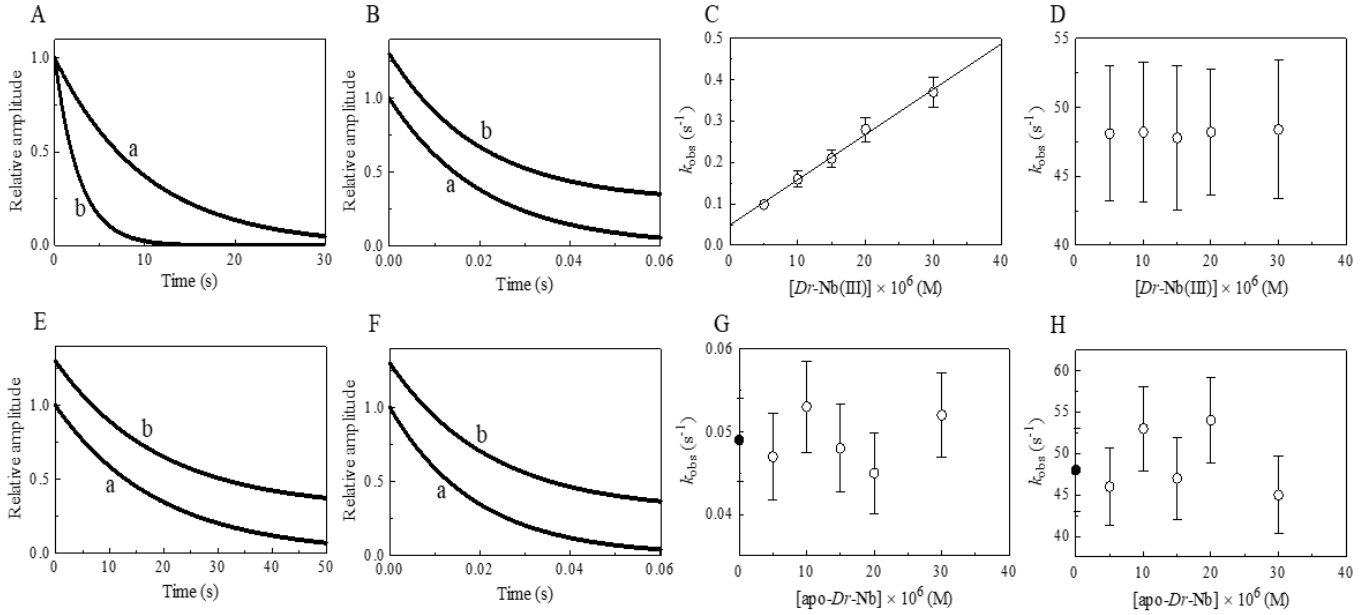

Figure 3. Effect of *Dr*-Nb(III) on the kinetics for peroxynitrite isomerization, at pH 8.5 and 22.0 °C. (**A**) Averaged time courses of the *Dr*-Nb(III)-catalyzed isomerization of peroxynitrite in the absence of CO_2. The time course analysis according to Equation (1) allowed us to determine the following values of k_{obs}: trace a, 1.0×10^{-1} s^{-1}, $R = 0.998$; trace b, 3.7×10^{-1} s^{-1}, $R = 0.999$. The *Dr*-Nb(III) concentration was: trace a, 1.0×10^{-5} M; trace b, 3.0×10^{-5} M. (**B**) Averaged time courses of the *Dr*-Nb(III)-catalyzed isomerization of peroxynitrite in the presence of CO_2. The time course analysis according to Equation (1) allowed us to determine the following values of k_{obs}: trace a, 4.8×10^{1} s^{-1}, $R = 0.999$; trace b, 4.8×10^{1} s^{-1}, $R = 0.998$. The *Dr*-Nb(III) concentration was: trace a, 1.0×10^{-5} M; trace b, 3.0×10^{-5} M. The CO_2 concentration was 1.2×10^{-3} M. For clarity, trace b has been up-shifted of 0.3 units. (**C**) Dependence of k_{obs} on the concentration of *Dr*-Nb(III) in the absence of CO_2. Data were analyzed according to Equation (2) with values of $k_{on} = 1.1 \times 10^{4}$ M^{-1} s^{-1} and $k_0 = 4.9 \times 10^{-2}$; $R = 0.995$, $p = 0.0002$. (**D**) Dependence of k_{obs} on the concentration of *Dr*-Nb(III) in the presence of CO_2. (**E**) Averaged time courses of peroxynitrite isomerization by apo-*Dr*-Nb in the absence of CO_2. The time course analysis according to Equation (1) allowed us to determine the following values of k_{obs}: trace a, 5.3×10^{-2} s^{-1}; trace b, 5.2×10^{-2} s^{-1}. The apo-*Dr*-Nb concentration was: trace a, 1.0×10^{-5} M; trace b, 3.0×10^{-5} M. For clarity, trace b has been up-shifted of 0.3 units. (**F**) Averaged time courses of peroxynitrite isomerization by apo-*Dr*-Nb in the presence of CO_2. The time course analysis according to Equation (1) allowed us to determine the following values of k_{obs}: trace a, 5.3×10^{1} s^{-1}; trace b, 4.5×10^{1} s^{-1}. The apo-*Dr*-Nb concentration was: trace a, 1.0×10^{-5} M; trace b, 3.0×10^{-5} M. For clarity, trace b has been up-shifted of 0.3 units. The CO_2 concentration was 1.2×10^{-3} M. (**G**) Dependence of k_{obs} on the concentration of apo-*Dr*-Nb in the absence of CO_2. The symbol on the ordinate indicates the value of k_0: 4.9×10^{-2} s^{-1}. The average value of k_{obs} obtained in the presence of apo-*Dr*-Nb is: 4.9×10^{-2} s^{-1}. (**H**) Dependence of k_{obs} on the concentration of apo-*Dr*-Nb in the presence of CO_2. The symbol on the ordinate indicates the value of k_0: 4.8×10^{1} s^{-1}. The average value of k_{obs} obtained in the presence of apo-*Dr*-Nb and CO_2 is 4.9×10^{1} s^{-1}. In panels D, G, and H the differences among the k_{obs} values are not statistically significant. The peroxynitrite concentration was 2.0×10^{-4} M. The HCO_3^- concentration was 5.0×10^{-1} M. Where not shown, the standard deviation is smaller than the symbol.

The analysis of the data shown in Figures 1–3 (panels C and D), according to Equation (2), allowed us to determine the values of k_{on} and k_0, corresponding to the slope and the *y*-intercept of the linear plots, respectively (Table 1). Moreover, the values of k_0 were measured in the absence of *Dr*-Nb(III) via the rapid mixing of the peroxynitrite solution with the appropriate Bis-Tris propane buffer solution (Figures 1–3, panels E and F). Both in the absence and presence of CO_2, the values of k_0 obtained by the different methods match well with each other (Table 1) and agree well with those previously reported [12,13,25,27,28,30,33,34,36,39,54] (see Table 2).

Table 1. Effect of pH and CO_2 on the values of k_{on} and k_0 for *Dr*-Nb(III)-induced isomerization of peroxynitrite at 22.0 °C [a].

pH	− CO_2		+ CO_2	
	k_{on} (M^{-1} s^{-1})	k_0 (s^{-1})	k_{on} (M^{-1} s^{-1})	k_0 (s^{-1})
5.8	$(2.2 \pm 0.3) \times 10^5$	$(8.1 \pm 0.8) \times 10^{-1}$	$(2.8 \pm 0.3) \times 10^5$	4.1 ± 0.4
7.0	$(4.7 \pm 0.5) \times 10^4$	$(3.1 \pm 0.3) \times 10^{-1}$	n.d.	$(1.5 \pm 0.2) \times 10^1$
8.5	$(1.1 \pm 0.1) \times 10^4$	$(4.9 \pm 0.5) \times 10^{-2}$	n.d.	$(4.8 \pm 0.5) \times 10^1$

[a] The CO_2 concentration was 1.2×10^{-3} M. 5.0×10^{-2} M Bis-Tris propane buffer. n.d., not determined.

Table 2. Effect of pH and CO_2 on values of k_{on} and k_0 for heme-protein-induced isomerization of peroxynitrite.

Heme-Protein	− CO_2		+ CO_2	
	k_{on} (M^{-1} s^{-1})	k_0 (s^{-1})	k_{on} (M^{-1} s^{-1})	k_0 (s^{-1})
Ma-Pgb(III) [a]	3.8×10^4	2.8×10^{-1}	n.d.	n.d.
Mt-trHbN(III) [b]	6.2×10^4	2.7×10^{-1}	n.d.	n.d.
Ph-trHbO(III) [c]	2.9×10^4	2.8×10^{-1}	n.d.	n.d.
Cj-trHbP(III) [d]	9.6×10^5	3.0×10^{-1}	8.8×10^5	2.1×10^1
Efc-Mb(III) [e]	2.9×10^4	3.5×10^{-1}	7.7×10^4	1.7×10^1
Pc-Mb(III) [f]	1.6×10^4	n.d.	n.d.	n.d.
Hs-Hb(III) [e]	1.2×10^4	3.0×10^{-1}	3.9×10^4	1.7×10^1
Mt-Nb(III) [g]	6.9×10^4	2.6×10^{-1}	n.d.	n.d.
At-Nb(III) [g]	3.7×10^4	3.0×10^{-1}	n.d.	n.d.
Dr-Nb(III) [h]	4.7×10^4	3.1×10^{-1}	n.d.	1.5×10^1
Hs-Nb(III) [i]	3.4×10^4	2.6×10^{-1}	n.d.	n.d.

[a] pH 7.4 and 20.0 °C. From [55]. [b] pH 7.0 and 20.0 °C. From [34]. [c] pH 7.0 and 20.0 °C. From [35]. [d] pH 7.3 and 25.0 °C. From [36]. [e] pH 7.0 and 20.0 °C. From [25]. [f] pH 7.5 and 20.0 °C. From [27]. [g] pH 7.2 and 25.0 °C. From [40]. [h] pH 7.0 and 22.0 °C. Present study. [i] pH 7.1 and 25.0 °C. From [39]. n.d., not determined.

As shown in Table 1, the values of k_{on} for the interaction between *Dr*-Nb(III) and peroxynitrite were unaffected by $CO_2/HCO_3^-/CO_3^{2-}$, suggesting that $CO_2/HCO_3^-/CO_3^{2-}$ does not alter the binding properties of *Dr*-Nb(III). The values of k_{on} for peroxynitrite isomerization via all-α-helical globins and all-β-barrel nitrobindins ranged between 1.2×10^4 M^{-1} s^{-1} for *Hs*-Hb(III) [25] and 6.9×10^4 M^{-1} s^{-1} for *Mt*-Nb(III) [40] (Table 2), suggesting that the very different structural organization [40,57–61] is not at the root of the different rate of peroxynitrite isomerization. However, the coordination of the heme-Fe(III) atom, the in- or out-of-plane position of the metal with respect to the pyrrole nitrogen atoms of the porphyrin, the ligand accessibility of the heme-Fe(III) atom, and its Lewis acidity may tune the kinetics of the related peroxynitrite decomposition [36].

To outline the role of the metal center, the values of k_{obs} have been determined as a function of (i) apo-*Dr*-Nb concentration (at a fixed peroxynitrite concentration) and (ii) peroxynitrite concentration (at fixed *Dr*-Nb(III) concentration). Apo-*Dr*-Nb does not induce the isomerization of peroxynitrite; in fact, the values of k_{obs} and k_0 match each other in the presence of apo-*Dr*-Nb (Figures 1–3, panels E–H), as reported for apo-*Efc*-Mb, apo-*Hs*-Hb, and apo-*Hs*-Nb [25,39]. As shown in Figure 4, the values of k_{obs} slightly decrease with an increasing peroxynitrite concentration, reflecting either the slow isomerization process of peroxynitrite-peroxynitrous acid dimers or their slow dissociation preceding the *Dr*-Nb(III)-catalyzed isomerization of peroxynitrite [30,36].

As shown in Figures 1–3 (panel D) and in Figure 4 (panel B) it turns out that, in the presence of 5.0×10^{-1} M $CO_2/HCO_3^-/CO_3^{2-}$, the role of *Dr*-Nb(III) in characterizing the rate constant of peroxynitrite isomerization becomes progressively less relevant as the pH is raised since values of k_0 for peroxynitrite isomerization obtained in the presence of $CO_2/HCO_3^-/CO_3^{2-}$ are faster by about two orders of magnitude than those obtained in its absence (Table 1). This indicates that $CO_2/HCO_3^-/CO_3^{2-}$ dramatically speeds up the

decay of peroxynitrite through direct interaction, without interfering with peroxynitrite binding to *Dr*-Nb(III) [9,12,13,25,27,28,30,32–34,36].

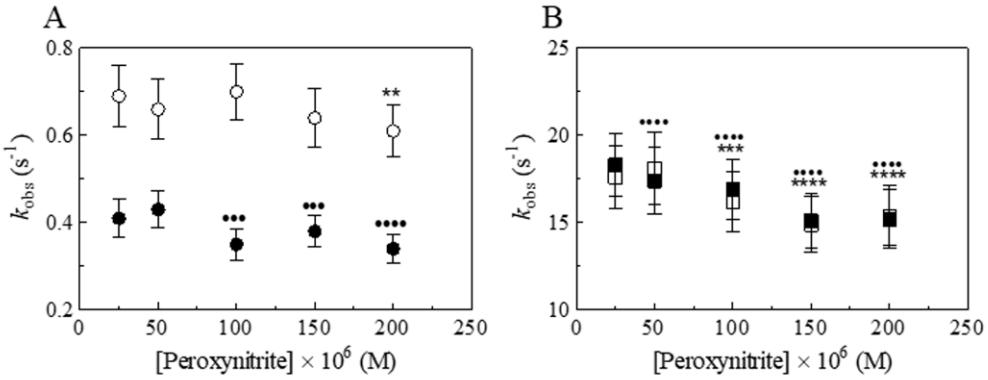

Figure 4. Effect of peroxynitrite concentration on the values of k_{obs} for the isomerization of peroxynitrite by *Dr*-Nb(III) and apo-*Dr*-Nb in the absence and presence of CO_2, at pH 7.0 and 22.0 °C. (**A**) Dependence of k_{obs} on the peroxynitrite concentration in the presence of *Dr*-Nb(III) (open circles) and apo-*Dr*-Nb (filled circles), in the absence of CO_2 (One-way ANOVA: open circles, ** $p < 0.01$, 25×10^{-6} M versus 200×10^{-6} M; filled circles, ••• $p < 0.001$, 25×10^{-6} M versus 100×10^{-6} M and versus 150×10^{-6} M, •••• $p < 0.0001$, 25×10^{-6} M versus 200×10^{-6} M). (**B**) Dependence of k_{obs} on the peroxynitrite concentration in the presence of *Dr*-Nb(III) (open squares) and apo-*Dr*-Nb (filled squares), in the presence of CO_2 (One-way ANOVA: open squares, *** $p < 0.001$, 25×10^{-6} M versus 100×10^{-6} M, **** $p < 0.0001$, 25×10^{-6} M versus 150×10^{-6} M and versus 200×10^{-6} M; filled squares, •••• $p < 0.0001$, 25×10^{-6} M versus 50×10^{-6} M, 100×10^{-6} M, 150×10^{-6} M, and 200×10^{-6} M). The *Dr*-Nb(III) and apo-*Dr*-Nb(III) concentration was 5.0×10^{-6} M. The HCO_3^- concentration was 5.0×10^{-1} M.

To clarify the differential roles of various ferric heme proteins and $CO_2/HCO_3^-/CO_3^{2-}$ levels in peroxynitrite detoxification, the overall effect of pH and $CO_2/HCO_3^-/CO_3^{2-}$ on the observed rate of peroxynitrite isomerization was investigated. Thus, the protonation equilibria of $OONO^-$/HOONO and $CO_2/HCO_3^-/CO_3^{2-}$ were considered. The effect of CO_2 on peroxynitrite isomerization in the absence of heme proteins (i.e., k_{obs}) can be described by Equation (3):

$$k_{obs} = \left(\frac{K_P}{[H^+]+K_P}\right) \times \left\{k_0 + [L] \times \left(\frac{k_{c1} \times [H^+]^2 + k_{c2} \times K_{c1} \times [H^+] + k_{c3} \times K_{c1} \times K_{c2}}{[H^+]^2 + K_{c1} \times [H^+] + K_{c1} \times K_{c1}}\right)\right\} + + \left(\frac{[H^+]}{[H^+]+K_P}\right) \times \left\{k_0^H + [L] \times \left(\frac{k_{c1}^H \times [H^+]^2 + k_{c2}^H \times K_{c1} \times [H^+] + k_{c3}^H \times K_{c1} \times K_{c2}}{[H^+]^2 + K_{c1} \times [H^+] + K_{c1} \times K_{c2}}\right)\right\} \quad (3)$$

where k_0 and $k_0{}^H$ are the intrinsic degradation rates of $OONO^-$ and HOONO, respectively, $[H^+]$ (= 10^{-pH}) is the proton concentration, K_P (= ($[OONO^-] \times [H^+]$)/[HOONO]) is the protonation constant of peroxynitrite, [L] is the reactant concentration (in our case $[HCO_3^-] = 5.0 \times 10^{-1}$ M), K_{c1} ($[H_2O]$) (= ($[HCO_3^-] \times [H^+]$)/$[CO_2] = 10^{-6.34}$) is the protonation equilibrium constant between HCO_3^- and CO_2, K_{c2} (= ($[CO_3^{2-}] \times [H^+]$)/$[HCO_3^-] = 10^{-10.25}$) is the protonation equilibrium constant between CO_3^{2-} and HCO_3^-; k_{c1} and $k_{c1}{}^H$ are the second-order rate constants for the reaction of CO_2 with $OONO^-$ and HOONO, respectively, k_{c2} and $k_{c2}{}^H$ are the second-order rate constants for the reaction with HCO_3^- of $OONO^-$ and HOONO, respectively, and k_{c3} and $k_{c3}{}^H$ are the second-order rate constants for the reaction with CO_3^{2-} of $OONO^-$ and HOONO, respectively.

The pH-dependence of peroxynitrite degradation in the absence of $CO_2/HCO_3^-/CO_3^{2-}$ (i.e., [L] = 0, see Equation (3)), allowed us to determine the values of k_0 (= 3.0×10^{-2} s^{-1}), $k_0{}^H$ (= 8.3×10^{-1} s^{-1}) and K_P (= $10^{-6.8}$) (Figure 5, panel A), showing that HOONO decays to NO_3^- faster than $OONO^-$, with a $pK_a \approx 6.8$ [13,36]. On the other hand, as already outlined before [9,13,22,27,28,30,36,39], when $CO_2/HCO_3^-/CO_3^{2-}$ is present (i.e.,

[L] = 5.0×10^{-1} M), the rate of peroxynitrite degradation becomes much faster and increases with a rising pH (see Table 1 and [36]). Therefore, employing Equation (3) and knowing the values of K_{c1} and K_{c2} (see above), the pH dependence of peroxynitrite degradation (Figure 5, panel B) gives information on the different values of k_{ci} and k_{ci}^{H} (with i = 1, 2, 3). The inspection of Table 3 allows for the following considerations:

(i) k_{c1}, k_{c2}^{H}, and k_{c3}^{H} are not playing any role, likely because either one or both reactants are too scarcely populated over the pH range investigated for the pseudo-first-order rate constant to have a detectable value, which can then be considered as ≈ 0 s^{-1};

(ii) At pH $\leq$ 6.2, the peroxynitrite degradation rate is mostly characterized by the reaction between HOONO and CO_2, corresponding to $k_{c1}^{H} = 8.0$ M^{-1} s^{-1});

(iii) For 6.2 < pH < 8.2, the peroxynitrite degradation rate is mostly characterized by the reaction between $OONO^-$ and HCO_3^-, corresponding to $k_{c2} = 6.2 \times 10^1$ M^{-1} s^{-1};

(iv) For pH $\geq$ 8.2, the peroxynitrite degradation rate is mostly characterized by the reaction between $OONO^-$ and CO_3^{2-}, corresponding to $k_{c3} = 1.8 \times 10^3$ M^{-1} s^{-1}.

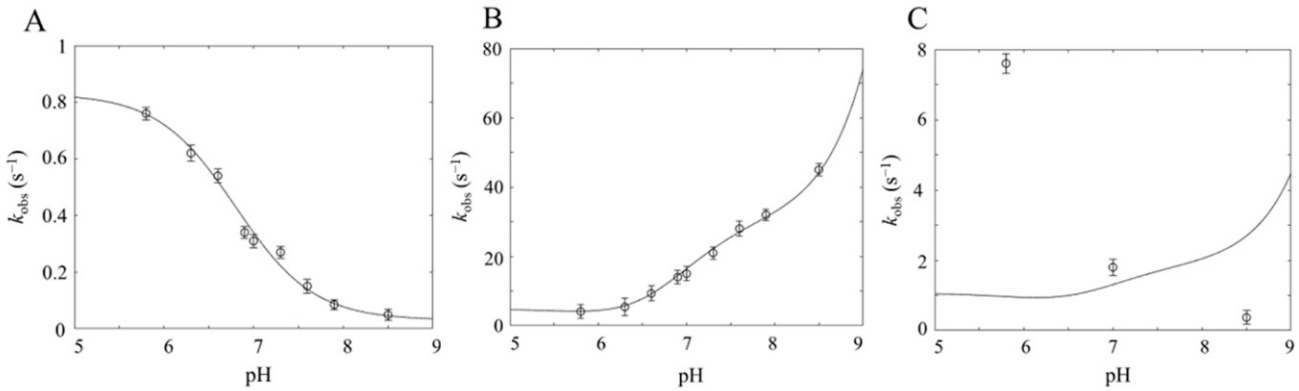

Figure 5. pH dependence of the peroxynitrite isomerization rate constant in the absence of $CO_2/HCO_3^-/CO_3^{2-}$ (**A**), in the presence of 5.0×10^{-1} M $CO_2/HCO_3^-/CO_3^{2-}$ (**B**), and in the presence of 3.0×10^{-2} M $CO_2/HCO_3^-/CO_3^{2-}$ (**C**). In all three panels, the continuous lines correspond to k_{obs}, as defined in Equation (3), under different conditions (i.e., [L] = 0 (**A**), [L] = 5.0×10^{-1} M (**B**), [L] = 3.0×10^{-2} M (**C**), employing the parameters reported in Table 3. In (**A**,**B**), the open circles correspond to experimental data obtained from the literature [36] on the peroxynitrite isomerization rate constants as a function of pH under the conditions described above. The continuous lines were obtained according to Equation (3) by the non-linear least-squares fitting of data. In (**C**), the open circles correspond to values of k_{obs} in the presence of 3.0×10^{-5} M *Dr*-Nb(III) in the absence of $CO_2/HCO_3^-/CO_3^{2-}$ at different pH values (present study). Data shown in (**C**) indicate that, at pH 5.8, the efficiency of the heme protein (at the indicated concentration) is higher than that of the $CO_2/HCO_3^-/CO_3^{2-}$ system, while at pH 8.5, the efficiency is lower.

Table 3. Values of the parameters fitting data with Equation (3).

Parameter	Value
k_0 (s^{-1})	$(3.0 \pm 0.5) \times 10^{-2}$
k_0^{H} (s^{-1})	$(8.3 \pm 1.0) \times 10^{-1}$
K_P (M)	$(1.6 \pm 0.3) \times 10^{-7}$
K_{c1} (M)	$(4.6 \pm 0.9) \times 10^{-7}$
K_{c2} (M)	$(5.6 \pm 1.2) \times 10^{-11}$
k_{c2} ($M^{-1}s^{-1}$)	$(6.2 \pm 1.3) \times 10^1$
k_{c3} ($M^{-1}s^{-1}$)	$(1.7 \pm 0.4) \times 10^3$
k_{c1}^{H} ($M^{-1}s^{-1}$)	8.0 ± 2.1

Obviously, the value of k_{obs} and its pH dependence depend on the $CO_2/HCO_3^-/CO_3^{2-}$ levels (i.e., [L]), envisaging that the relative levels of the ferric heme protein and $CO_2/HCO_3^-/CO_3^{2-}$ are crucial in defining the respective role for peroxynitrite detoxification. Of note,

data reported in Figures 1–3 (panel D) refer to $[CO_2/HCO_3^-/CO_3^{2-}] = 5.0 \times 10^{-1}$ M, while in the bloodstream, the physiological levels of $CO_2/HCO_3^-/CO_3^{2-}$ (~3.0×10^{-2} M) are about 10-20 fold lower. Therefore, under these conditions, k_{obs} decreases significantly even in the presence of $CO_2/HCO_3^-/CO_3^{2-}$, as indicated by Equation (3) (Figure 5, panel C). The pH-dependent mechanism of peroxynitrite degradation can be described by Scheme 2, which reports the different pathways for peroxynitrite degradation.

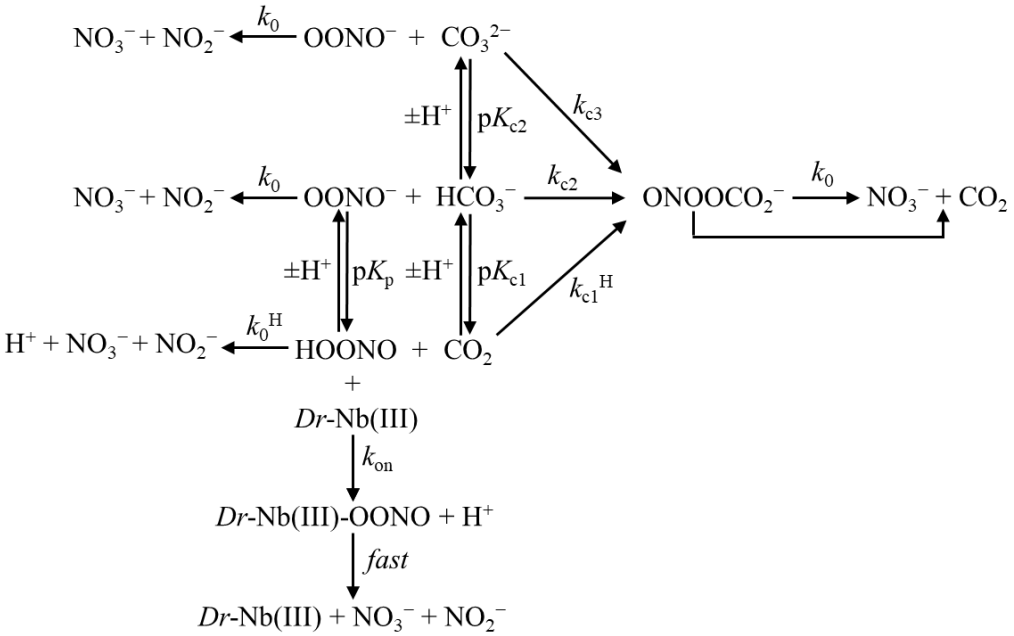

Scheme 2. Effect of pH on peroxynitrite degradation. The scheme reproduces the mechanism described by Equation (3), clarifying the meaning of the different parameters; only the significant parameters are reported (see text).

According to Equation (3), the effects of the heme protein and $CO_2/HCO_3^-/CO_3^{2-}$ levels were simulated (Figure 5, panel C), with the values of the rates at $[CO_2/HCO_3^-/CO_3^{2-}] = 3.0 \times 10^{-2}$ M and [*Dr*-Nb(III)] = 3.0×10^{-5} M (see Figures 1–3, panels C). At acidic pH values, the role of *Dr*-Nb(III) (= 3.0×10^{-5} M) is prevalent for peroxynitrite isomerization, while at a neutral pH the role of *Dr*-Nb(III) (= 3.0×10^{-5} M) is equivalent to that of the $CO_2/HCO_3^-/CO_3^{2-}$ system (Figure 5C). For alkaline pH values, *Dr*-Nb(III) levels higher than 3.0×10^{-5} M would be required to play a relevant role in peroxynitrite detoxification (see Figure 5, panel C).

The relative importance of the heme proteins and $CO_2/HCO_3^-/CO_3^{2-}$ catalyzing the peroxynitrite isomerization is crucial since, according to the literature [9,12,25,30,36,62,63], ferric heme proteins prevent L-tyrosine nitration, which, instead, occurs either in the presence of apo-*Dr*-Nb and/or of $CO_2/HCO_3^-/CO_3^{2-}$ (Figure 6) (see also Scheme 1). In fact, the relative yield of NO_3^- and NO_2^-, obtained from peroxynitrite isomerization catalyzed by *Dr*-Nb(III), ranged between 89 and 92%, and between 7 and 12%, respectively. However, in the absence of *Dr*-Nb(III) and/or in the presence of apo-*Dr*-Nb and/or $CO_2/HCO_3^-/CO_3^{2-}$, the values of the relative yield of NO_3^- and NO_2^- ranged between 69 and 74%, and between 7 and 12%, respectively (Table 4). The great relevance of these observations is confirmed by the fact that, under stressed conditions, zebrafish triggers a defense mechanism through nitrosative stress and peroxynitrite production for which its degradation may be, on one side, enhanced by the elevated levels of CO_2 [48,49], but, on the other side, inhibited by the consequent lowering of the pH level. In any event, the correlation between the peroxynitrite degradation by ferric heme proteins and CO_2 levels appears to be relevant within in vivo models of zebrafish, and it may have important consequences for the O_2 supply to poorly oxygenated tissues, such as the retina [50,51].

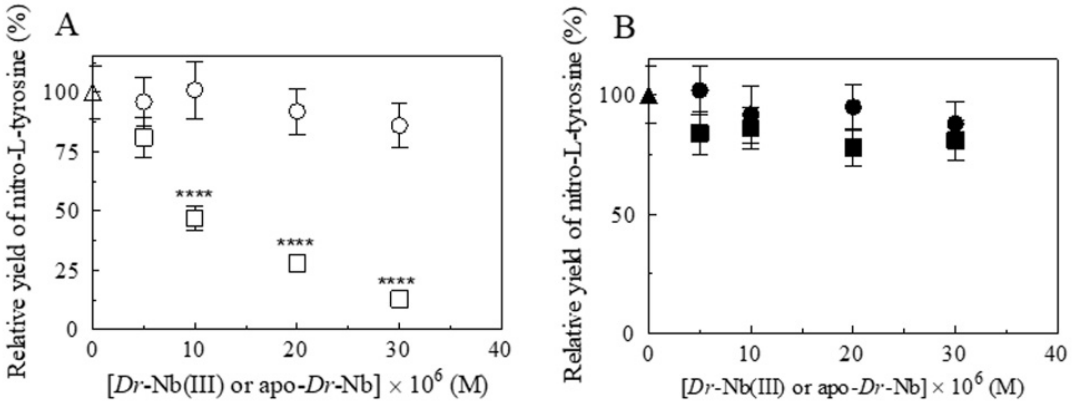

Figure 6. Effect of *Dr*-Nb on L-tyrosine nitrosylation induced from peroxynitrite, at pH 7.0 and 22.0 °C. (**A**) Dependence of the nitro-L-tyrosine yield on the *Dr*-Nb(III) (open squares) and apo-*Dr*-Nb (open circles) concentration in the absence of CO_2 (One-way ANOVA: open squares, **** $p < 0.0001$, 0 M versus 10×10^{-6} M, 20×10^{-6} M, and 30×10^{-6} M). (**B**) Dependence of the nitro-L-tyrosine yield on the *Dr*-Nb(III) (filled squares) and apo-*Dr*-Nb (filled circles) concentration in the presence of CO_2. The symbols on the *y*-axis (open and filled triangle) indicate the nitro-L-tyrosine yield in the absence and presence of CO_2, respectively. The L-tyrosine concentration was 1.0×10^{-4} M. The peroxynitrite concentration was 2.0×10^{-4} M. Where not shown, the standard deviation is smaller than the symbol.

Table 4. Percentage of NO_3^- and NO_2^- obtained from peroxynitrite isomerization at pH 7.0 and at 22.0 °C [a].

Dr-Nb(III)	Apo-*Dr*-Nb	CO_2	NO_3^-	NO_2^-
(M)	(M)	(M)	(%)	(%)
0.0	0.0	0.0	73 ± 8	28 ± 3
0.0	0.0	1.2×10^{-3}	69 ± 7	30 ± 3
0.0	3.5×10^{-5}	0.0	71 ± 8	29 ± 3
0.0	3.5×10^{-5}	1.2×10^{-3}	74 ± 7	25 ± 2
3.5×10^{-5}	0.0	0.0	89 ± 9	12 ± 2
3.5×10^{-5}	0.0	1.2×10^{-3}	93 ± 8	7 ± 1
3.5×10^{-5}	3.5×10^{-5}	0.0	91 ± 9	10 ± 1
3.5×10^{-5}	3.5×10^{-5}	1.2×10^{-3}	92 ± 9	8 ± 1

[a] The peroxynitrite concentration was 2.0×10^{-4} M; 5.0×10^{-2} M Bis-Tris propane buffer.

4. Conclusions

Ferric heme proteins and the $CO_2/HCO_3^-/CO_3^{2-}$ system are the major players in peroxynitrite detoxification, for which efficiency depends on both the concentration of these two actors and the pH level. CO_3^{2-} is much more effective at peroxynitrite inactivation, as compared to CO_2, with HCO_3^- displaying an intermediate activity. Of note, the CO_3^{2-} levels were much lower than those of the other two components in the system under physiological conditions. Although ferric heme proteins are intrinsically much more effective than the $CO_2/HCO_3^-/CO_3^{2-}$ system, their levels are usually significantly lower than $CO_2/HCO_3^-/CO_3^{2-}$. Since over the physiological pH range the rate of peroxynitrite detoxification by $CO_2/HCO_3^-/CO_3^{2-}$ (i.e., ~3.0×10^{-2} M) is ~1.5 s^{-1}, values of k_{obs} (= k_{on} × [heme-Fe(III)]), for peroxynitrite scavenging by ferric heme-proteins must be larger than 2 s^{-1}. Overall, only the level of the circulating *Hs*-Hb(III) (~2.0×10^{-4} M; corresponding to about 2–3% of the total *Hs*-Hb in red cells) appears to be sufficient to play a relevant role in the detoxification by peroxynitrite under physiological conditions.

Furthermore, it must be remarked that acidification, which often occurs in the bloodstream of fish when they dive to depth [64–66] and can even be magnified by increased levels of CO_2 [49], decreases the effect of the $CO_2/HCO_3^-/CO_3^{2-}$ system, rendering the role of ferric heme proteins even more crucial. This is especially important in the ocular sys-

tem and in the protection of the retina against oxidative stress linked to peroxynitrite [3,50]. Therefore, under specific environmental conditions (typical of diving fish), *Dr*-Nb(III) indeed may play a relevant physiological role in peroxynitrite scavenging from poorly oxygenated tissues, such as the retina.

Author Contributions: A.C. and G.D.S. performed experiments; A.d.M. supervised molecular biology experiments; P.A. and M.C. conceptualized and supervised biochemical experiments, formally analyzed the data, wrote reviewed and edited the manuscript. All authors have read and agreed to the published version of the manuscript.

Funding: G.D.S., A.d.M. and P.A. gratefully acknowledge the grant of Dipartimento di Eccellenza, MIUR, Roma Tre University (Legge 232/2016, Articolo 1, Comma 314-337). M.C. gratefully acknowledges the support of the Italian Ministry of Health and of Fondazione Roma.

Institutional Review Board Statement: Not applicable.

Informed Consent Statement: Not applicable.

Data Availability Statement: All the data will be available upon request to the corresponding authors.

Conflicts of Interest: The authors declare no conflict of interest.

References

1. Cantó, A.; Olivar, T.; Romero, F.J.; Miranda, M. Nitrosative Stress in Retinal Pathologies: Review. *Antioxidants* **2019**, *8*, 543. [CrossRef] [PubMed]
2. Ahmad, A.; Ahsan, H. Biomarkers of inflammation and oxidative stress in ophthalmic disorders. *J. Immunoass. Immunochem.* **2020**, *41*, 257–271. [CrossRef] [PubMed]
3. Lei, Y.; Gao, Y.; Song, M.; Cao, W.; Sun, X. Peroxynitrite is a novel risk factor and treatment target of glaucoma. *Nitric Oxide* **2020**, *99*, 17–24. [CrossRef] [PubMed]
4. Beckman, J.S.; Koppenol, W.H. Nitric oxide, superoxide, and peroxynitrite: The good, the bad, and ugly. *Am. J. Physiol.* **1996**, *271*, C1424–C1437. [CrossRef] [PubMed]
5. Ducrocq, C.; Blanchard, B.; Pignatelli, B.; Ohshima, H. Peroxynitrite: An endogenous oxidizing and nitrating agent. *Cell. Mol. Life Sci.* **1999**, *55*, 1068–1077. [CrossRef] [PubMed]
6. Clementi, E.; Nisoli, E. Nitric oxide and mitochondrial biogenesis: A key to long-term regulation of cellular metabolism. *Comp. Biochem. Physiol.* **2005**, *142*, 102–110. [CrossRef]
7. DeNicola, A.; Radi, R. Peroxynitrite and drug-dependent toxicity. *Toxicology* **2005**, *208*, 273–288. [CrossRef]
8. Pacher, P.; Beckman, J.S.; Liaudet, L. Nitric Oxide and Peroxynitrite in Health and Disease. *Physiol. Rev.* **2007**, *87*, 315–424. [CrossRef]
9. Goldstein, S.; Merényi, G. The Chemistry of Peroxynitrite: Implications for Biological Activity. *Methods Enzymol.* **2008**, *436*, 49–61. [CrossRef]
10. Jones, L.H. Chemistry and Biology of Biomolecule Nitration. *Chem. Biol.* **2012**, *19*, 1086–1092. [CrossRef]
11. Radi, R. Oxygen radicals, nitric oxide, and peroxynitrite: Redox pathways in molecular medicine. *Proc. Natl. Acad. Sci. USA* **2018**, *115*, 5839–5848. [CrossRef]
12. Goldstein, S.; Lind, J.; Merényi, G. Chemistry of peroxynitrites and peroxynitrates. *Chem. Rev.* **2005**, *105*, 2457–2470. [CrossRef]
13. Ascenzi, P.; Leboffe, L.; Santucci, R.; Coletta, M. Ferric microperoxidase-11 catalyzes peroxynitrite isomerization. *J. Inorg. Biochem.* **2015**, *144*, 56–61. [CrossRef]
14. Lymar, S.V.; Hurst, J.K. Rapid reaction between peroxynitrite ion and carbon dioxide: Implications for biological activity. *J. Am. Chem. Soc.* **1995**, *117*, 8867–8868. [CrossRef]
15. DeNicola, A.; Freeman, B.A.; Trujillo, M.; Radi, R. Peroxynitrite Reaction with Carbon Dioxide/Bicarbonate: Kinetics and Influence on Peroxynitrite-Mediated Oxidations. *Arch. Biochem. Biophys.* **1996**, *333*, 49–58. [CrossRef]
16. Bonini, M.G.; Radi, R.; Ferrer-Sueta, G.; Ferreira, A.M.D.C.; Augusto, O. Direct EPR Detection of the Carbonate Radical Anion Produced from Peroxynitrite and Carbon Dioxide. *J. Biol. Chem.* **1999**, *274*, 10802–10806. [CrossRef]
17. Radi, R.; Denicola, A.; Freeman, B.A. Peroxynitrite reactions with carbon dioxide-bicarbonate. *Methods Enzymol.* **1999**, *301*, 353–367. [CrossRef]
18. Meli, R.; Nauser, T.; Latal, P.; Koppenol, W.H. Reaction of peroxynitrite with carbon dioxide: Intermediates and determination of the yield of CO_3- and $NO_2\bullet$. *J. Biol. Inorg. Chem.* **2002**, *7*, 31–36. [CrossRef]
19. Squadrito, G.L.; Pryor, W.A. Mapping the reaction of peroxynitrite with CO_2: Energetics, reactive species, and biological im-plications. *Chem. Res. Toxicol.* **2002**, *15*, 885–895. [CrossRef]
20. Augusto, O.; Goldstein, S.; Hurst, J.K.; Lind, J.; Lymar, S.V.; Merenyi, G.; Radi, R. Carbon dioxide-catalyzed peroxynitrite reactivity—The resilience of the radical mechanism after two decades of research. *Free Radic. Biol. Med.* **2019**, *135*, 210–215. [CrossRef]

21. Augusto, O.; Truzzi, D.R. Carbon dioxide redox metabolites in oxidative eustress and oxidative distress. *Biophys. Rev.* **2021**, *13*, 889–891. [CrossRef]
22. Mehl, M.; Daiber, A.; Herold, S.; Shoun, H.; Ullrich, V. Peroxynitrite reaction with heme proteins. *Nitric Oxide* **1999**, *3*, 142–152. [CrossRef]
23. Shimanovich, R.; Groves, J.T. Mechanisms of Peroxynitrite Decomposition Catalyzed by FeTMPS, a Bioactive Sulfonated Iron Porphyrin. *Arch. Biochem. Biophys.* **2001**, *387*, 307–317. [CrossRef] [PubMed]
24. Jensen, M.P.; Riley, D.P. Peroxynitrite Decomposition Activity of Iron Porphyrin Complexes. *Inorg. Chem.* **2002**, *41*, 4788–4797. [CrossRef] [PubMed]
25. Herold, S.; Shivashankar, K. Metmyoglobin and Methemoglobin Catalyze the Isomerization of Peroxynitrite to Nitrate. *Biochemistry* **2003**, *42*, 14036–14046. [CrossRef] [PubMed]
26. Herold, S.; Fago, A.; Weber, R.E.; Dewilde, S.; Moens, L. Reactivity studies of the Fe(III) and Fe(II)NO forms of human neu-roglobin reveal a potential role against oxidative stress. *J. Biol. Chem.* **2004**, *279*, 22841–22847. [CrossRef] [PubMed]
27. Herold, S.; Kalinga, S.; Matsui, A.T.; Watanabe, Y. Mechanistic Studies of the Isomerization of Peroxynitrite to Nitrate Catalyzed by Distal Histidine Metmyoglobin Mutants. *J. Am. Chem. Soc.* **2004**, *126*, 6945–6955. [CrossRef]
28. Herold, S.; Puppo, A. Kinetics and mechanistic studies of the reactions of metleghemoglobin, ferrylleghemoglobin, and nitrosyl-leghemoglobin with reactive nitrogen species. *J. Biol. Inorg. Chem.* **2005**, *10*, 946–957. [CrossRef]
29. Ascenzi, P.; Visca, P. Scavenging of Reactive Nitrogen Species by Mycobacterial Truncated Hemoglobins. *Methods Enzymol.* **2008**, *436*, 317–337. [CrossRef]
30. Ascenzi, P.; di Masi, A.; Coletta, M.; Ciaccio, C.; Fanali, G.; Nicoletti, F.P.; Smulevich, G.; Fasano, M. Ibuprofen impairs allo-sterically peroxynitrite isomerization by ferric human serum heme-albumin. *J. Biol. Chem.* **2009**, *284*, 31006–31017. [CrossRef]
31. Ascenzi, P.; Bolli, A.; Di Masi, A.; Tundo, G.R.; Fanali, G.; Coletta, M.; Fasano, M. Isoniazid and rifampicin inhibit allosterically heme binding to albumin and peroxynitrite isomerization by heme–albumin. *J. Biol. Inorg. Chem.* **2010**, *16*, 97–108. [CrossRef]
32. Ascenzi, P.; Ciaccio, C.; Sinibaldi, F.; Santucci, R.; Coletta, M. Cardiolipin modulates allosterically peroxynitrite detoxification by horse heart cytochrome c. *Biochem. Biophys. Res. Commun.* **2011**, *404*, 190–194. [CrossRef]
33. Ascenzi, P.; Ciaccio, C.; Sinibaldi, F.; Santucci, R.; Coletta, M. Peroxynitrite detoxification by horse heart carboxymethylated cytochrome c is allosterically modulated by cardiolipin. *Biochem. Biophys. Res. Commun.* **2011**, *415*, 463–467. [CrossRef]
34. Ascenzi, P.; Coletta, A.; Cao, Y.; Trezza, V.; Leboffe, L.; Fanali, G.; Fasano, M.; Pesce, A.; Ciaccio, C.; Marini, S.; et al. Isoniazid Inhibits the Heme-Based Reactivity of Mycobacterium tuberculosis Truncated Hemoglobin N. *PLoS ONE* **2013**, *8*, e69762. [CrossRef]
35. Coppola, D.; Giordano, D.; Tinajero-Trejo, M.; di Prisco, G.; Ascenzi, P.; Poole, R.K.; Verde, C. Antarctic bacterial haemoglobin and its role in the protection against nitrogen reactive species. *Biochim. Biophys. Acta* **2013**, *1834*, 1923–1931. [CrossRef]
36. Ascenzi, P.; Pesce, A. Peroxynitrite scavenging by Campylobacter jejuni truncated hemoglobin P. *J. Biol. Inorg. Chem.* **2017**, *22*, 1141–1150. [CrossRef]
37. Ascenzi, P.; Coletta, M. Peroxynitrite Detoxification by Human Haptoglobin:Hemoglobin Complexes: A Comparative Study. *J. Phys. Chem. B* **2018**, *122*, 11100–11107. [CrossRef]
38. Coppola, D.; Giordano, D.; Milazzo, L.; Howes, B.D.; Ascenzi, P.; di Prisco, G.; Smulevich, G.; Poole, R.K.; Verde, C. Coex-istence of multiple globin genes conferring protection against nitrosative stress to the Antarctic bacterium Pseudoalteromonas haloplanktis TAC125. *Nitric Oxide* **2018**, *73*, 39–51. [CrossRef]
39. De Simone, G.; di Masi, A.; Polticelli, F.; Ascenzi, P. Human nitrobindin: The first example of an all-β-barrel ferric heme-protein that catalyzes peroxynitrite detoxification. *FEBS Open Bio* **2018**, *8*, 2002–2010. [CrossRef]
40. De Simone, G.; Di Masi, A.; Vita, G.M.; Polticelli, F.; Pesce, A.; Nardini, M.; Bolognesi, M.; Ciaccio, C.; Coletta, M.; Turilli, E.S.; et al. Mycobacterial and Human Nitrobindins: Structure and Function. *Antioxidants Redox Signal.* **2020**, *33*, 229–246. [CrossRef]
41. Giordano, D.; Pesce, A.; Vermeylen, S.; Abbruzzetti, S.; Nardini, M.; Marchesani, F.; Berghmans, H.; Seira, C.; Bruno, S.; Luque, F.J.; et al. Structural and functional properties of Antarctic fish cytoglobins-1: Cold-reactivity in multi-ligand reactions. *Comput. Struct. Biotechnol. J.* **2020**, *18*, 2132–2144. [CrossRef] [PubMed]
42. Radi, R.; Beckman, J.S.; Bush, K.M.; Freeman, B.A. Peroxynitrite oxidation of sulfhydryls. The cytotoxic potential of superoxide and nitric oxide. *J. Biol. Chem.* **1991**, *266*, 4244–4250. [CrossRef]
43. Gow, A.; Duran, D.; Thom, S.R.; Ischiropoulos, H. Carbon dioxide enhancement of peroxynitrite mediated protein tyrosine nitration. *Arch. Biochem. Biophys.* **1996**, *333*, 42–48. [CrossRef] [PubMed]
44. Scorza, G.; Minetti, M. One electron oxidation pathway of thyols by peroxynitrite in biological fluids: Bicarbonate and ascorbate promote the formation of albumin disulphide dimers in human blood plasma. *Biochem. J.* **1998**, *329*, 405–413. [CrossRef]
45. Bonini, M.G.; Augusto, O. Carbon Dioxide Stimulates the Production of Thiyl, Sulfinyl, and Disulfide Radical Anion from Thiol Oxidation by Peroxynitrite. *J. Biol. Chem.* **2001**, *276*, 9749–9754. [CrossRef]
46. Augusto, O.; Bonini, M.G.; Amanso, A.M.; Linares, E.; Santos, C.C.; De Menezes, S.L. Nitrogen dioxide and carbonate radical anion: Two emerging radicals in biology. *Free Radic. Biol. Med.* **2002**, *32*, 841–859. [CrossRef]
47. Elks, P.M.; van der Vaart, M.; van Hensbergen, V.; Schutz, E.; Redd, M.J.; Murayama, E.; Spaink, H.P.; Meijer, A.H. Myco-bacteria counteract a TLR-mediated nitrosative defense mechanism in a zebrafish infection model. *PLoS ONE* **2014**, *9*, e100928. [CrossRef]

48. Shahab, M.; Rosati, R.; Meyer, D.N.; Shields, J.N.; Crofts, E.; Baker, T.R.; Jamesdaniel, S. Cisplatin-induced hair cell loss in zebrafish neuromasts is accompanied by protein nitration and Lmo4 degradation. *Toxicol. Appl. Pharmacol.* **2020**, *410*, 115342. [CrossRef]
49. Vossen, L.E.; Jutfelt, F.; Cocco, A.; Thörnqvist, P.-O.; Winberg, S. Zebrafish (*Danio rerio*) behavior is largely unaffected by el-evated pCO_2. *Conserv. Physiol.* **2016**, *4*, cow065. [CrossRef]
50. Damsgaard, C. Physiology and evolution of oxygen secreting mechanism in the fisheye. *Comp. Biochem. Physiol. Part A Mol. Integr. Physiol.* **2020**, *252*, 110840. [CrossRef]
51. Tummanapalli, S.S.; Kuppusamy, R.; Yeo, J.H.; Kumar, N.; New, E.J.; Willcox, M.D. The role of nitric oxide in ocular surface physiology and pathophysiology. *Ocul. Surf.* **2021**, *21*, 37–51. [CrossRef]
52. De Simone, G.; Tundo, G.R.; Coletta, A.; Coletta, M.; Ascenzi, P. Hydroxylamine-induced oxidation of ferrous nitrobindins. *J. Biol. Inorg. Chem.* **2022**, *27*, 443–453. [CrossRef]
53. Antonini, E.; Brunori, M. *Hemoglobin and Myoglobin in Their Reactions with Ligands*; North Holland Publishing Co.: Amsterdam, The Netherlands; London, UK, 1971.
54. Herold, S.; Exner, M.; Boccini, F. The Mechanism of the Peroxynitrite-Mediated Oxidation of Myoglobin in the Absence and Presence of Carbon Dioxide. *Chem. Res. Toxicol.* **2003**, *16*, 390–402. [CrossRef]
55. Ascenzi, P.; Leboffe, L.; Pesce, A.; Ciaccio, C.; Sbardella, D.; Bolognesi, M.; Coletta, M. Nitrite-Reductase and Peroxynitrite Isomerization Activities of Methanosarcina acetivorans Protoglobin. *PLoS ONE* **2014**, *9*, e95391. [CrossRef]
56. Miranda, K.M.; Espey, M.G.; Wink, D.A. A Rapid, Simple Spectrophotometric Method for Simultaneous Detection of Nitrate and Nitrite. *Nitric Oxide* **2001**, *5*, 62–71. [CrossRef]
57. Perutz, M.F. Regulation of Oxygen Affinity of Hemoglobin: Influence of Structure of the Globin on the Heme Iron. *Annu. Rev. Biochem.* **1979**, *48*, 327–386. [CrossRef]
58. Bolognesi, M.; Bordo, D.; Rizzi, M.; Tarricone, C.; Ascenzi, P. Nonvertebrate hemoglobins: Structural bases for reactivity. *Prog. Biophys. Mol. Biol.* **1997**, *68*, 29–68. [CrossRef]
59. Bianchetti, C.M.; Blouin, G.C.; Bitto, E.; Olson, J.S.; Phillips, G.N., Jr. The structure and NO binding properties of the nitro-phorin-like heme-binding protein from *Arabidopsis thaliana* gene locus At1 g79260.1. *Proteins* **2010**, *78*, 917–931. [CrossRef]
60. Bianchetti, C.M.; Bingman, C.A.; Phillips, G.N., Jr. Structure of the C-terminal heme-binding domain of THAP domain con-taining protein 4 from Homo sapiens. *Proteins* **2011**, *79*, 1337–1341. [CrossRef]
61. Ascenzi, P.; Brunori, M. A molecule for all seasons: The heme. *J. Porphyrins Phthalocyanines* **2016**, *20*, 134–149. [CrossRef]
62. Kissner, R.; Koppenol, W.H. Product Distribution of Peroxynitrite Decay as a Function of pH, Temperature, and Concentration. *J. Am. Chem. Soc.* **2001**, *124*, 234–239. [CrossRef] [PubMed]
63. Ascenzi, P.; Bocedi, A.; Visca, P.; Minetti, M.; Clementi, E. Does CO_2 modulate peroxynitrite specificity? *IUBMB Life* **2006**, *58*, 611–613. [CrossRef] [PubMed]
64. Brunori, M. Molecular Adaptation to Physiological Requirements: The Hemoglobin System of Trout. *Curr. Top. Cell. Regul.* **1975**, *9*, 1–39. [CrossRef] [PubMed]
65. Brunori, M.; Coletta, M.; Giardina, B.; Wyman, J. A macromolecular transducer as illustrated by trout hemoglobin IV. *Proc. Natl. Acad. Sci. USA* **1978**, *75*, 4310–4312. [CrossRef]
66. Ciaccio, C.; Coletta, A.; Coletta, M. Role of hemoglobin structural-functional relationships in oxygen transport. *Mol. Asp. Med.* **2021**, *84*, 101022. [CrossRef]